technologies

MDPI

Article

Electrospinning of Chitosan–Halloysite Nanotube Biohybrid Mats for Clobetasol Propionate Delivery

Natallia V. Dubashynskaya [1], Valentina A. Petrova [1], Igor V. Kudryavtsev [2], Andrey S. Trulioff [2], Artem A. Rubinstein [2], Alexey S. Golovkin [3], Alexander I. Mishanin [3], Anton A. Murav'ev [1], Iosif V. Gofman [1], Daria N. Poshina [1] and Yury A. Skorik [1,*]

[1] Branch of Petersburg Nuclear Physics Institute Named by B.P. Konstantinov of National Research Centre «Kurchatov Institute»-Institute of Macromolecular Compounds, Bolshoi VO 31, St. Petersburg 199004, Russia
[2] Institute of Experimental Medicine, Acad. Pavlova 12, St. Petersburg 197022, Russia
[3] Almazov National Medical Research Centre, Akkuratova 2, St. Petersburg 197341, Russia
* Correspondence: yury_skorik@mail.ru

Abstract: The application of electrospinning technologies for the preparation of mats based on mucoadhesive polysaccharides, such as chitosan (CS), is an attractive strategy for the development of biopolymeric delivery systems for topical corticosteroids. In this work, an electrospinning technique is described for the preparation of CS-based mats doped with halloysite nanotubes (HNTs) with modified release of clobetasol propionate (CP). The optimized composition of the electrospinning solution was determined: 2.4% solution of CS in 46% acetic acid with addition of PEO (10% of CS mass) and HNTs (5% of CS mass); CP was introduced as an ethanol solution at the rate of 2 mg CP per 1 g of the obtained nonwoven material. The process parameters (the electrospinning voltage of 50–65 kV, the rotation speed of the spinning electrode of 10 min^{-1}, and the distance between the electrodes of 24 cm) were also optimized. The developed technology allowed us to obtain homogeneous nanofiber mats with excellent mechanical properties and biphasic drug release patterns (66% of CP released within 0.5 h and 88% of CP released within 6 h). The obtained nanofiber mats maintained the anti-inflammatory activity of corticosteroid at the level of free CP and showed no cytotoxicity.

Keywords: chitosan; halloysite nanotubes; clobetasol propionate; electrospun mats; oromucosal drug delivery systems; anti-inflammatory activity

check for updates

Academic Editor: Manoj Gupta

Received: 10 December 2024
Revised: 23 January 2025
Accepted: 19 February 2025
Published: 21 February 2025

Citation: Dubashynskaya, N.V.; Petrova, V.A.; Kudryavtsev, I.V.; Trulioff, A.S.; Rubinstein, A.A.; Golovkin, A.S.; Mishanin, A.I.; Murav'ev, A.A.; Gofman, I.V.; Poshina, D.N.; et al. Electrospinning of Chitosan–Halloysite Nanotube Biohybrid Mats for Clobetasol Propionate Delivery. *Technologies* **2025**, *13*, 90. https://doi.org/10.3390/technologies13030090

Copyright: © 2025 by the authors. Licensee MDPI, Basel, Switzerland. This article is an open access article distributed under the terms and conditions of the Creative Commons Attribution (CC BY) license (https://creativecommons.org/licenses/by/4.0/).

1. Introduction

Fibrous mucoadhesive mats based on natural polymers obtained by electrospinning are promising for local oromucosal delivery of anti-inflammatory drugs due to their flexibility and large surface area, which allows them to firmly adhere to the oral mucosa and effectively deliver therapeutic agents to the damaged sites [1,2]. The 3D structure of electrospun mats mimics the biological structure and functions of tissues, which has a positive effect on the regeneration of damaged tissues and accelerates injury healing [3].

The incorporation of bioactive agents into the nanofiber 3D mesh is an effective strategy for in situ drug delivery, which expands the potential for biomedical applications of electrospun materials [4]. The route of drug delivery influences its therapeutic effect, namely pharmacokinetics, biodistribution, metabolism, and toxicity. One of the advantages of using biopolymer nanofiber mats as mucoadhesive drug delivery systems is the possibility of topical application to the pathological site, which reduces the systemic toxicity of the drug [5]. Various technological strategies can be used to program and control the rate and

time of drug release. For example, drugs can be incorporated into nanofibers both by direct mixing with the spinning solution and by immobilization on the surface of the nanofibers, thereby allowing modification of the drug release profile [3].

Various strategies to manipulate the structure of nanofibers have been developed to improve the efficiency of drug delivery using nonwoven materials. For example, it has been shown in [6] that highly oriented poly(lactic-co-glycolic acid) (PLGA) nanofibers (spatial orientation > 99%) provide a sustained release of dexamethasone. In vitro testing showed that the aligned fibers had less burst release and more sustained release compared to the random fibers. One of the ways to provide more sustained and prolonged drug release is to form core–shell type nanofibers by coaxial electrospinning [7] and using emulsions as electrospinning solution [8].

The use of biopolymers in the development of electrospun mats is of interest because of their excellent advantages over conventional polymers. Biopolymers are characterized by biodegradability, biocompatibility, and non-toxicity, which is extremely important for the development of materials for biomedical applications, especially for drug delivery. Materials with tailored functional properties (e.g., strength and elasticity, modified drug release, biodegradability, etc.) can be obtained by combining different biopolymers [9,10]. For example, Wan et al. [11] obtained smooth fibers by co-electrospinning poly(ε-caprolactone) and keratin. The functional groups of keratin were then used to covalently conjugate the biopolymer heparin, which was then used to bind vascular endothelial growth factor (VEGF). The developed mats were effective in accelerating the proliferation of human umbilical vein endothelial cells while inhibiting the growth of human umbilical artery smooth muscle cells due to the combined action of VEGF and heparin. The presence of heparin also reduced proteolytic degradation of VEGF and promoted the sustained release of VEGF.

Another strategy to improve the mechanical and biopharmaceutical properties of electrospun mats is the use of nanofillers of different nature, such as nanocellulose and disintegrated bacterial cellulose fibers [12,13], chitin nanowhiskers [14,15], silicate nanoparticles [16,17], metal and metal oxide nanoparticles, etc. [18–20]. Among inorganic nanofillers for biopolymer nonwoven matrices, halloysite clay nanotubes (HNTs) are of great interest due to their biocompatibility and low toxicity. HNTs are unique porous aluminosilicates that have been widely used as multifunctional and chemically adaptable nanocomposite fillers to create innovative and smart materials with modified drug release, as well as fillers for antimicrobial nanocomposite materials, scaffolds for tissue engineering, adsorbents for environmental and biomedical applications, etc. [21–24]. The HNTs are characterized by a wide range of lengths (50 nm to 30 μm) and outer and inner diameters (20–600 nm and 5–150 nm, respectively) [25]. The hollow tubular structure of HNTs provides a large specific surface area and uniform distribution in polymer matrices to enhance mechanical properties and thermal stability. The large specific surface area of HNTs allows them to form a network that interpenetrates the polymer matrix and limits the mobility of macromolecules, as well as provides load distribution during matrix stretching, which increases stress [26].

The presence of -OH groups provides functionalization of the HNT surface via the formation of various bonds (e.g., hydrogen bonds and electrostatic interactions) with functional groups of both biopolymers and drug molecules [21]. The internal cavity of HNTs is positively charged and the external surface is negatively charged (in the pH range of 2.5–8.5) due to the positive and negative ζ-potential of alumina and silica, respectively. Therefore, HNTs can be excellent nanocontainers for loading or adsorbing drug molecules on the surface to achieve programmable and controlled drug release [25,27]. For example, Tohidi et al. [26] obtained a composite nanofiber mat based on PLGA and chitosan (CS) doped

with HNTs loaded with the antibiotic amoxicillin. It was shown that the incorporation of HNTs did not significantly change the morphology of the nanofibers but significantly improved the mechanical properties of the material (the ultimate stress was 8 MPa and the strain was 40%, while for pure CS and PLGA matrices the ultimate stresses were about 2.3 and 7.4 MPa, respectively). Furthermore, the incorporation of HNTs into the electrospun matrix reduced the initial burst release of amoxicillin and provided its modified release (about 22% of the drug was released in 10 h, with a cumulative release of about 50% of amoxicillin in 40 h).

Nonwoven materials based on the biocompatible and nontoxic polysaccharide CS are promising materials for the manufacture of oromucosal delivery systems for anti-inflammatory agents, including corticosteroids [28,29]. CS nonwoven mats are characterized by excellent mucoadhesion and can be securely attached to the mucosa [30]. Also, CS has an affinity for hydrophobic compounds with sterane structure and is capable of adsorbing steroids, cholesterol, etc. [31,32]. The incorporation of PEO and HNTs into the spinning solution can be used to improve the electrospinning process of CS, which enhances the physical and mechanical properties of the nanofibers; both PEO and HNTs affect the structure of the spinning solution and subsequently the drug release profile [33,34].

Topical corticosteroids are recommended as a first-line treatment of non-malignant oral mucosal pathologies due to the minimization of systemic side effects. Clobetasol propionate (CP) belongs to the group of high-potency topical corticosteroids and is widely used for the symptomatic treatment of inflammatory and immunopathologies of the oral mucosa in the form of ointments, gels, and lotions. However, the reduced residence time on the mucosa is the main drawback of these traditional dosage forms [35–38]. Therefore, the incorporation of the topical corticosteroid CP for oromucosal administration into electrospun mats based on mucoadhesive natural polysaccharides CS is of interest. We hypothesize that the use of HNTs will allow the formation of a reinforcing network due to the interaction of nanotubes with negatively charged surface with protonated amino groups of CS, providing the possibility to obtain the material with high strength properties (also in wet state), as well as to modify the CP release.

2. Materials and Methods

2.1. Materials

Crab shell CS with viscosity-average molecular weight (Mη) of 60,000 and degree of deacetylation (DDA) of 84% was purchased from Bioprogress Ltd. (Shchelkovo, Russia). The Mark–Houwink equation ($[\eta] = 3.41 \times 10^{-3} \times M_\eta^{1.02}$) was used to determine the M_η. The characteristic viscosity ([η] = 2.56 dL/g) was determined in a 0.33 M acetic acid/0.3 M NaCl solvent at 20 °C using the Ubbelohde viscometer (Design Bureau Pushchino, Pushchino, Russia) [39]. The DDA was determined by ^{1}H NMR spectroscopy on a Bruker Avance 400 spectrometer (Bruker, Billerica, MA, USA) at 70 °C. HNTs (Figure 1) with an average diameter of 40–130 nm and a length of 0.5–1.2 μm, purchased from Natural Nano (Rochester, NY, USA). PEO (molecular weight of 900,000) and CP were purchased from Sigma-Aldrich (St. Louis, MO, USA); all other reagents were analytical grade and were used as received.

2.2. Fabrication of Biocomposite Mats by Electrospinning Technique

To prepare the 100.0 g electrospinning solution, 2.4 g CS was first dispersed in 23.6 g water under vigorous stirring for several hours, and then 46.0 g glacial acetic acid was added under continuous stirring. Then, 8.0 g of 3% aqueous PEO solution was added to the resulting CS solution, making the PEO mass 10% of the CS mass. Then, 20.0 g of 0.6% aqueous dispersion of HNTs was added under continuous vigorous stirring, and the mass

of HNTs was 5% of the mass of CS. For uniform distribution of HNTs in the CS solution, the aqueous HNT dispersion was prepared as follows: HNTs were dispersed in distilled water for 1 day and then sonicated at 20 W power for 10 min using a Bandelin Sonopuls mini 20 probe ultrasonicator (Bandelin Electronics, Berlin, Germany) and stabilized with 0.2% CS solution under continuous sonication. CP (2 mg CP per 1 g of nonwoven mat) was added as a 0.03% ethanol solution (20.0 g).

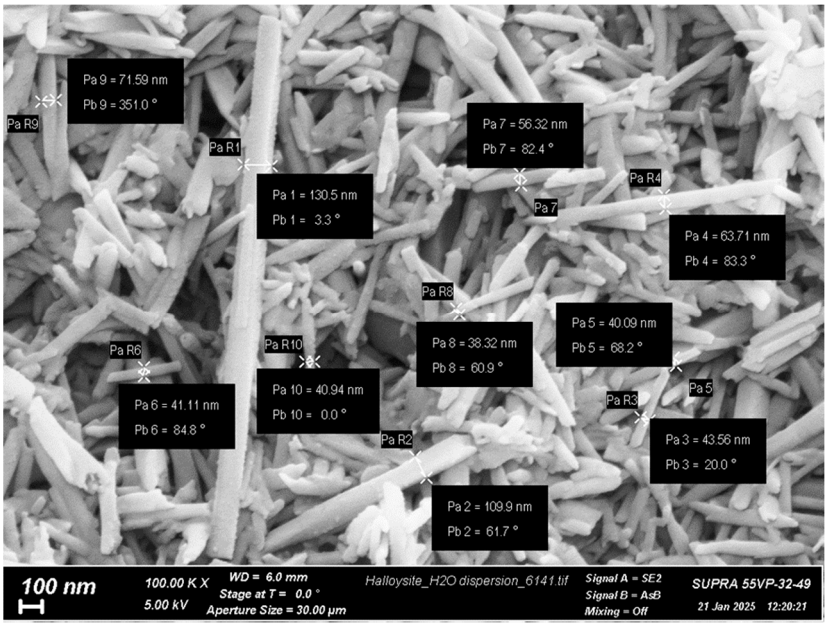


Figure 1. SEM image of the native HNTs (SUPRA-55VP scanning electron microscope, Carl Zeiss, Oberkochen, Germany).

The non-capillary electrospinning process was performed using a Nanospider NS Lab 500 instrument (Elmarco, Liberec, Czech Republic). To ensure stability and uniformity of the solution jets, the electrospinning voltage was adjusted from 50 to 65 kV. The rotation speed of the spinning electrode was set to 10 min^{-1}, with a distance of 24 cm between the electrodes. A paper support was used to collect the fibers. After the electrospinning process, the samples were stored at room temperature for a period of 5 days and then heated to 80 °C for a period of 3 h to remove acetic acid and to convert CS to the basic form, which ensures the insolubility of the material in water and physiological conditions. The resulting electrospun mat (CS-HNT) contained 80 wt% CS, 4 wt% HNT, and 16 wt% PEO. The CP content in the CS-HNT-CP mat was 2 mg/g.

The CP-free (CS-0) and the CP-containing (CS-CP) CS-based mats were also prepared using the same procedure but without the HNT introduction step.

2.3. Electrospun Mat Characterization

The average fiber diameter was determined from the SEM images. Images were obtained using a Phenom G Pro instrument (Phenom-World BV, Eindhoven, The Netherlands). Approximately 500 fiber diameters were evaluated for each sample and diameter distributions were obtained.

The swelling capacity of the electrospun mats in water and physiological solution (0.9% NaCl) was determined gravimetrically according to the following equation:

$$\text{Swelling capacity} = \frac{(\text{Ws} - \text{Wd})}{\text{Wd}} \quad (1)$$

where Wd is the weight of the dry mat; Ws is the weight of the swollen mat.

The mechanical properties of the electrospun mats were investigated using an AG-100 kNX Plus setup (Shimadzu, Kyoto, Japan). The setup was operated in uniaxial extension mode. According to the requirements of ASTM D638, strip-shaped samples (2 × 30 mm) were stretched at a rate of 20 mm/min at room temperature. During the tests, the stress–strain curves of the samples were recorded. Young's modulus (E), the yield stress (σ_y), the break stress (σ_b), and the ultimate deformation (ε_b) were determined. All measurements were performed in triplicate and the resulting data were averaged.

2.4. Drug Release Kinetics

A sample of the mat (10 mg) was placed in a dissolution medium (2.5 mL) and then incubated at 37 °C. The dissolution medium used was a salivary fluid simulator (SFS with pH 6.8) prepared by dissolving 8.00 g sodium chloride, 0.19 g monobasic potassium phosphate, and 2.38 g dibasic sodium phosphate in 1 L distilled water; if necessary, the pH of the resulting solution was adjusted to 6.8 [40]. At certain time intervals, 2 mL of the medium was withdrawn for CP quantification; the dissolution medium was replenished with fresh SFS. A UV-1700 PharmaSpec spectrophotometer (Shimadzu, Kyoto, Japan) was used to determine the amount of CP released at a wavelength of 242 nm using a calibration curve.

2.5. In Vitro Study of Cytotoxicity and Anti-Inflammatory Activity on the THP-1 Cell Line Model

To determine the cytotoxicity and immune response of monocytes and macrophages, we used acute monocytic leukemia cells (THP-1 cell line) obtained from the vertebrate cell culture collection of the Institute of Cytology of the Russian Academy of Sciences. THP-1 cells were cultured as described in [41].

To study the anti-inflammatory activity of CP, we used an in vitro cell-based model of inflammation–activation of THP-1 cells with tumor necrosis factor-α (TNFα), we studied the effects of the prepared samples (corresponding to a CP concentration of 1 μg/mL) on TNFα-induced CD54 expression by these cells, and we detected viable and apoptotic cells by YO-PRO-1/PI staining, as described previously [41].

2.6. In Vitro Study of Cytotoxicity and Adhesion on the MSC Model

The adhesion of mesenchymal stromal cells (MSCs), derived from the visceral adipose tissue of healthy male Wistar rats, was used to assess the cell adhesion properties and cytotoxicity of the materials. This study was conducted in accordance with the ethical standards set forth by the Commission for the Control of Care and Use of Laboratory Animals at Almazov National Medical Research Centre (protocol No. 21-12PZ#V3, 13 July 2021). The experimental methodology followed previously published procedures [19,42].

3. Results and Discussion

3.1. Electrospinning of Composite CS-HNT and CS-HNT-CP Mats

The compositions of the electrospinning solutions were chosen based on preliminary studies [43]. The solution components, such as acetic acid, PEO, HNTs, and ethanol, are all known to increase the spinnability of CS. We span a range of solutions using the voltage of the first stable spin as an indicator of solution spinnability. The solutions contained 2% CS, 20% PEO by mass of CS, 50% acetic acid, 20% ethanol, and a range of HNT concentrations. In this case, the voltage of the first stable spin was the same for all solutions, 23 kV (Table 1). Therefore, we can conclude that the key role in spinnability is played by the high concentration of acetic acid. It was previously shown that ethanol increases the spinnability of CS in dilute acids at a concentration of 20% [43]. Indeed, when the acid concentration

was reduced to 5%, solutions without ethanol were not spinnable, and for solutions with ethanol, a dependence on the concentration of HNTs was observed (Table 1).

Table 1. Spinnability of solutions by the voltage of the first stable spinning.

Solution Composition	HNTs, % (by Weight of CS)	Voltage, kV
2% CS, 20% PEO (by CS mass), 50% acetic acid	2 4 6 8	23
2% CS, 20% PEO (by CS mass), 50% acetic acid, 20% ethanol	2 4 6 8	23
2% CS, 20% PEO (by CS mass), 5% acetic acid	2 4 6 8	not spinable
2% CS, 20% PEO (by CS mass), 5% acetic acid, 20% ethanol	2 4 6 8	45 25 35 44

For the final compositions, a high concentration of acetic acid was chosen to neutralize the influence of the remaining components on the formation process and fiber thickness. Based on the data obtained, the compositions of the electrospinning blends and the parameters of the spinning process were optimized (Section 2.2).

Since HNTs have a negatively charged outer surface, the 0.01% aqueous dispersion of HNTs was stabilized with a low concentration of 0.2% CS solution under continuous sonication to prevent aggregation with the concentrated electrospinning solution of polycationic CS and to achieve uniform distribution of the nanofiller. The resulting materials, CS-HNT (control) and CS-HNT-CP (spun with ethanol solution of CP), had identical fiber diameter distributions and very close values of mean fiber diameter (Figure 2).

3.2. Swelling of Electrospun Mats

Swelling is an important property of oromucosal solid dosage forms, including electrospun nonwoven mats, that affects their mucoadhesive ability to the mucosa as well as the drug release profile. In the presence of oral fluid, the CS-based mat swells to form a hydrogel layer, resulting in the release and activation of mucoadhesive CS groups capable of forming chemical bonds and physical entanglements with mucin macrochains. The swelling of the biopolymer mat ensures free diffusion of drug molecules for their complete release [44]. The swelling capacity of the obtained mats (CS-CP, CS-HNT, and CS-HNT-CP) in water and in 0.9% NaCl solution is presented in Table 2.

The introduction of CP ethanol solution into the electrospinning solution promoted a slight increase in the degree of swelling of the nonwoven material (CS-CP and CS-HNT-CP) in both water and the physiological solution compared to the CS-HNT mat, which is apparently related to the rearrangement of intermolecular hydrogen bonds when ethanol is added to the acetic acid solution of CS, leading to a change in the intermolecular interactions in the resulting mats. The introduction of nanofillers into the CP-containing mat did not reduce its swelling capacity (compare CS-CP and CS-HNT-CP), indicating that the CS-HNT-CP formulation is promising for oromucosal delivery.

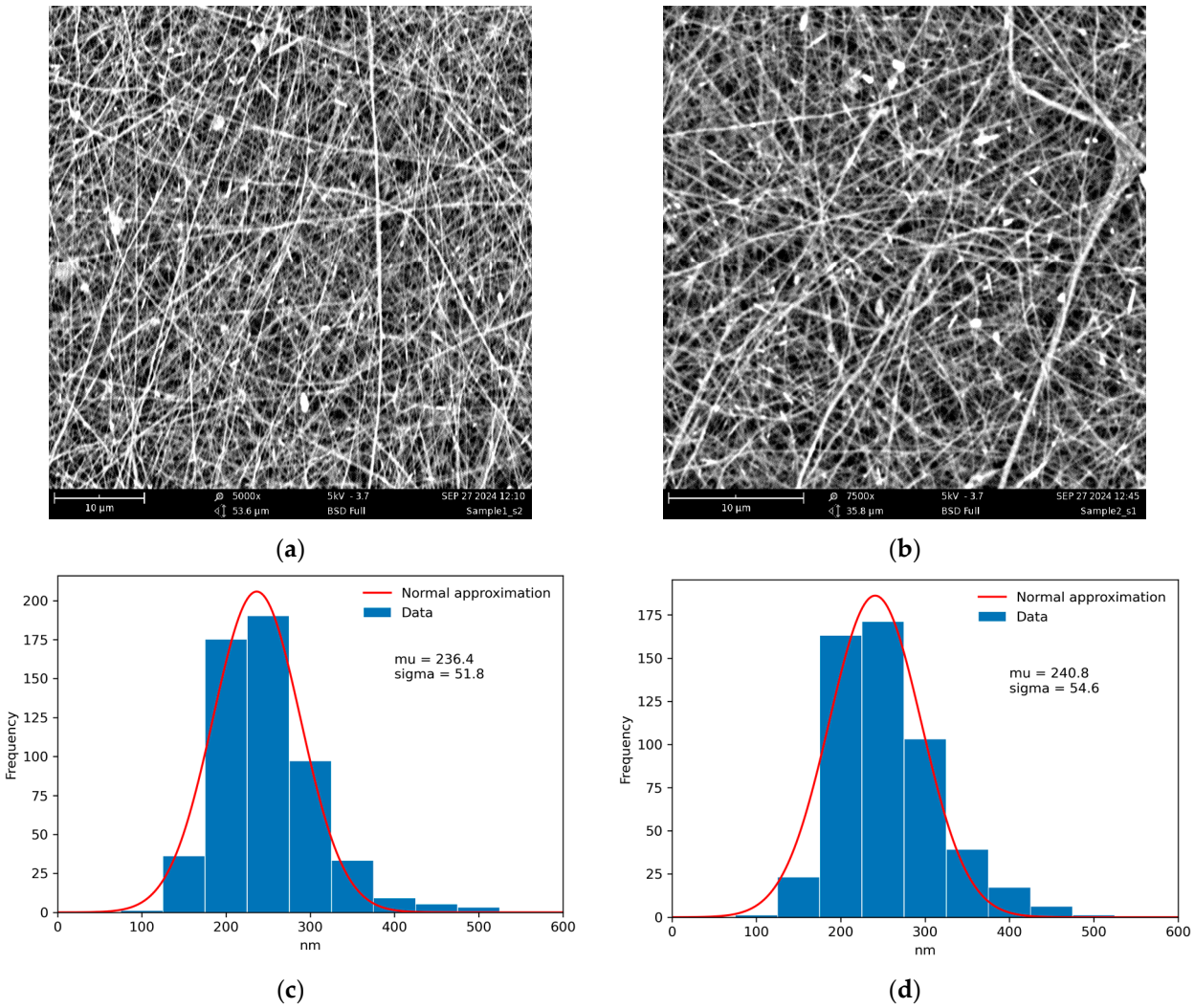


Figure 2. SEM images of the CS-HNT (**a**), CS-HNT-CP (**b**) nanofibers, and corresponding fiber diameter distributions (**c**,**d**). The distributions were obtained using ImageJ software (Version 1.54 K).

Table 2. The swelling degree of electrospun materials.

Sample	Swelling Capacity (g/g)	
	In Water	In 0.9% NaCl Solution
CS-CP	3.7	3.5
CS-HNT	3.1	2.7
CS-HNT-CP	3.6	3.4

3.3. Mechanical Properties of Electrospun Mats

The CS-based nonwovens containing PEO, HNTs, and CP, as well as the combination of these components, have reasonable mechanical properties (Table 3).

Table 3. Mechanical properties of the electrospun mats.

Sample	E (MPa)	σ_y, (MPa)	σ_b (MPa)	ε_b (%)
CS-0	398 ± 9	9.4 ± 0.4	10.1 ± 0.8	6.2 ± 0.8
CS-HNT	546 ± 65	12.1 ± 0.3	14.3 ± 0.9	5.9 ± 0.3
CS-CP	620 ± 85	11.9 ± 0.8	15.3 ± 0.7	10.3 ± 0.3
CS-HNT-CP	632 ± 56	12.2 ± 0.9	16.2 ± 1.2	11.0 ± 2.0

It is well known that PEO is added to the CS solution to enhance the electrospinning capability and improve the strength properties of the material [33]. The introduction of high-modulus rod-like HNTs into the CS matrix resulted in the formation of a rigid framework in the material volume, which effectively absorbed the applied mechanical loads. In addition, HNTs contain a large amount of hydroxyl groups, making the surface negatively charged, which facilitates interactions with the positively charged polymer matrix, resulting in composites with superior properties [45].

The addition of CP ethanol solution to the electrospinning composite solution used for the production of CS-HNT electrospun mats helps to maintain the strength of the nonwoven material and increase its elasticity, which is associated with the influence of ethyl alcohol. According to a number of works, it is known that the addition of ethanol to the CS solution changes the system of intermolecular bonds and affects the supramolecular structure of the solution, which can subsequently affect the physical and mechanical properties of CS-based materials and the drug release profile [46,47]. Regarding the nature of the deformation process (Figure 3), the nonwoven CS-HNT is similar to CS-HNT-CP.

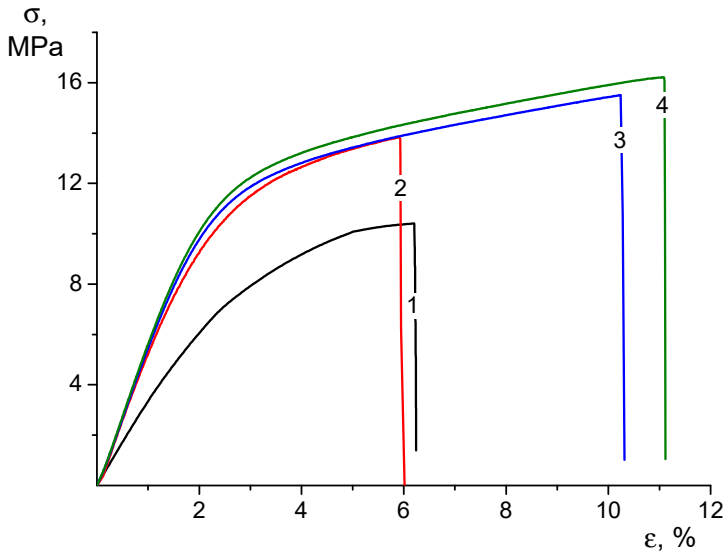


Figure 3. Stress–strain curves of CS-0 (1), CS-HNT (2), CS-CP (3), and CS-HNT-CP (4) electrospun mats.

However, based on the increased deformability of the CS-HNT-CP material containing both HNTs and CP, it can be assumed that the introduction of ethanol to the electrospinning solution leads to a change in the surface properties of the nanofibers. In fact, the destruction of such nonwoven materials is realized due to the disruption of the bonds between individual fibers combined with the destruction of the fibers themselves. The results obtained indicate that in the nonwoven material containing CP, both mechanisms are realized with less intensity than in the CS-HNT formulation, which leads to an increase in the ultimate deformation by almost 2 times compared to the CS-HNT material and, consequently, to an increase in the strength (Figure 3).

While discussing the properties of the materials under consideration, it should be mentioned that these mats are intended for practical applications mainly in the swollen state. Therefore, it would be interesting to evaluate the mechanical properties of the mats subjected to swelling in water. The results are shown in Table 4 and Figure 4.

Table 4. Mechanical properties of the electrospun mats in the swollen state.

Sample	E (MPa)	σ_y, (MPa)	σ_b (MPa)	ε_b (%)
CS-CP	13.3 ± 0.9	-	5.1 ± 0.5	18 ± 1
CS-HNT-CP	17.8 ± 0.9	-	7.1 ± 0.8	25 ± 1

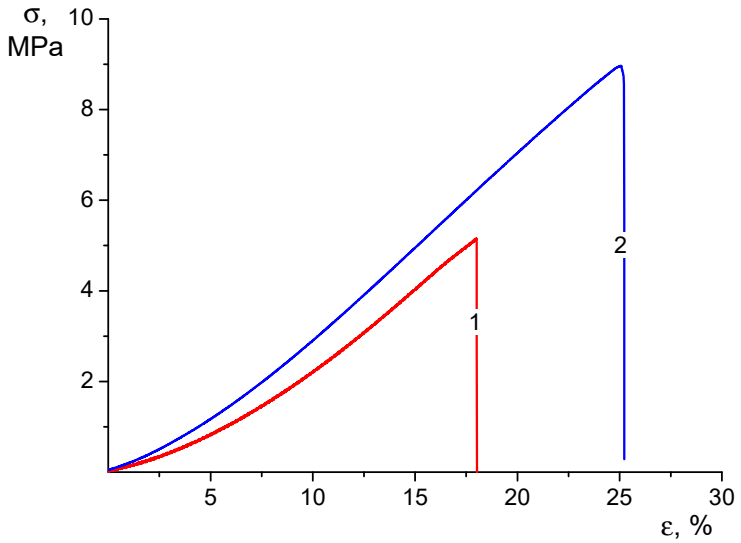


Figure 4. Stress–strain curves of CS-CP (1) and CS-HNT-CP (2) electrospun mats in the swollen state.

When analyzing these results, it should first be noted that swelling caused a profound change in the qualitative appearance of the stress–strain curves of the tested materials (compare Figures 3 and 4). In the process of tensile stretching of swollen nonwoven materials, the stress grows monotonically as the strain increases with a successive increase in the value of d_σ/d_ε. Therefore, it is not possible to determine the yield strength from the strain curve.

Swelling results in a significant (2–3 times) increase in the ultimate strain before the material fails. At the same time, the strength of swollen materials decreases about twice as much as the strength of dry mats but remains quite sufficient for practical use of the swollen material: by the value of this characteristic, swollen mats are close to low-density polyethylene films.

3.4. Release Kinetics of CP from the CS-HNT-CP Mat

In vitro studies have shown that the CS-based nonwoven doped with HNTs (CS-HNT-CP) provides a modified drug release profile compared to the HNT-free mat (Figure 5). The HNT-free mat (CS-CP) was characterized by rapid CP release (about 80–90% of the drug was released within 0.5–1 h). In the case of the HNT-containing mat (CS-HNT-CP), two phases are observed on the kinetic curve: (1) an initial burst release of CP (66% of CP is released within 0.5 h) and (2) a subsequent sustained release of CP (88% of CP is released within 6 h) (Figure 5). This two-phase drug release profile is explained by the high initial release of CP located on the surface of the highly porous nanofibrous material. The delayed release of CP is apparently ensured both by the effects of the interaction of the HNT network with the protonated amino groups of CS and by hydrogen bonds between CS and PEO, which are described for CS/PEO blends in a ratio of about 4:1 [48]. In addition, CP can be incorporated into the nanofiber during its formation by electrospinning.

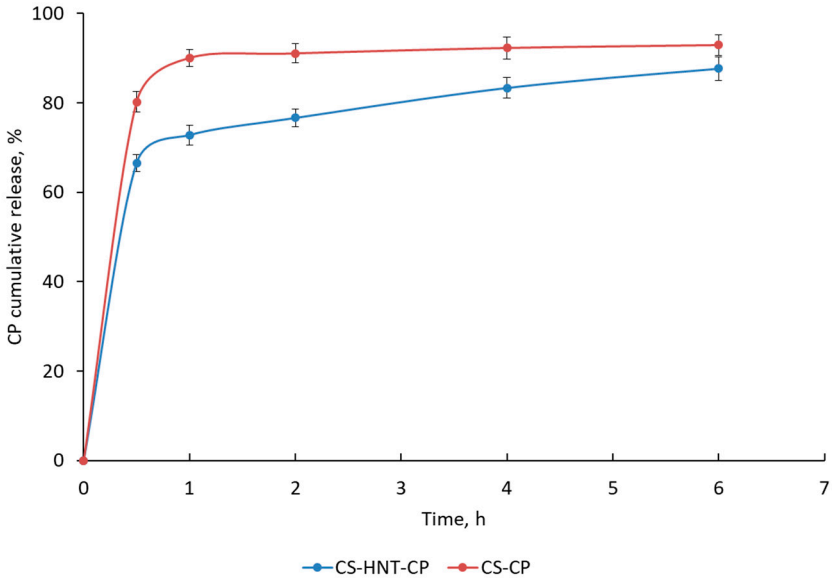


Figure 5. Cumulative CP release in SFS (pH 6.8) at 37 °C. Data are presented as the mean of three measurements ± standard deviation.

3.5. In Vitro Study of Cytotoxicity and Anti-Inflammatory Activity

To study the cytotoxicity and anti-inflammatory activity of CP loaded into a HNT-doped CS-based polymer electrospun mat, we used the THP-1 cell line, which is one of the most widely used models to study the immune response of monocytes and macrophages to activation by pro-inflammatory agents, including the pro-inflammatory cytokine TNFα. The results of the study of the potential toxic effects of composite nonwoven mats with CP, as well as CP-free samples and a solution of free CP (equivalent to 1 μg/mL CP) on THP-1 cell lines are presented in Table 5. It was shown that the relative cell viability in the presence of the polymer mats was not significantly different from the control, indicating that the developed materials did not exhibit cytotoxicity.

Table 5. Relative viability of YO-PRO-1-PI stained THP-1 cell line after 24 h incubation. Data ($n \geq 4$) are presented as median and interquartile range, Me (Q25; Q75).

Sample	Without Addition of TNFα	With the Addition of 10 ng/mL TNFα
Negative control	95.92 (95.23; 96.45)	94.44 (94.30; 94.59)
CP	95.57 (94.37; 96.66)	93.90 (91.78; 95.89)
CS-HNT-CP	96.14 (95.67; 96.63)	94.75 (94.03; 95.64)
CS-HNT	95.80 (94.65; 96.75)	93.74 (91.55; 95.18)

Next, the anti-inflammatory activity of the biopolymer samples was evaluated by their effect on the blockade of THP-1 cell activation. The addition of TNFα at a final concentration of 10 ng/mL was accompanied by an activation of THP-1 cell lines, which was expressed as an increase in the expression level of CD54 on the cell membrane (0.583 MFI versus 1.929 MFI at $p < 0.001$) (Table 6). In addition, both CP-containing mat and CP-free mat significantly reduced TNFα-induced CD54 expression on the cell membrane (from 1.929 MFI to 0.933 MFI and 1.106 MFI, respectively, at $p < 0.05$ in both cases). It should also be noted that the values obtained for the THP-1 cell line under the influence of TNFα significantly exceeded the values of the samples without TNFα stimulation for both CS-HNT-CP and CS-HNT mats and for the free CP solution.

Table 6. Effect of CS-NHT-CP and CS-HNT on the activation level of THP-1 cell line. Data ($n \geq 4$) are presented as MFI as median and interquartile range, Me (Q25; Q75).

Sample	Without Addition TNFα	With the Addition of 10 ng/mL TNFα
Negative control	0.583 (0.543; 0.596) *	1.929 (1.735; 2.420) *
CP	0.616 (0.607; 0.657)	0.931 (0.846; 1.090)
CS-HNT-CP	0.566 (0.540; 0.574)	0.933 (0.899; 1.015) **
CS-HNT	0.567 (0.565; 0.579)	1.106 (0.986; 1.341) **

* Differences with negative control are significant at $p < 0.001$ according to the non-parametric Mann–Whitney test; ** Differences with THP-1 with addition of TNFα are significant at $p < 0.05$ according to the non-parametric Mann–Whitney test.

3.6. In Vitro Study of Cytotoxicity and Cell Adhesion

It was found that both the investigated electrospun mats and coverslip (control) contained adherent cells with typical morphology. The MSCs on the coverslips represented a confluent/sub-confluent monolayer of evenly distributed, elongated cells with multiple syncytium-like structures; cells in the process of mitosis were also observed. Microfilaments of cell actin were clearly visible as longitudinal structures stained in red. However, in the experimental samples (CS-HNT and CS-HNT-CP), rounded cells with few outgrowths and with diffuse cytoplasmic staining were observed. It can be concluded that such cells were in a state of apoptosis (Figure 6).

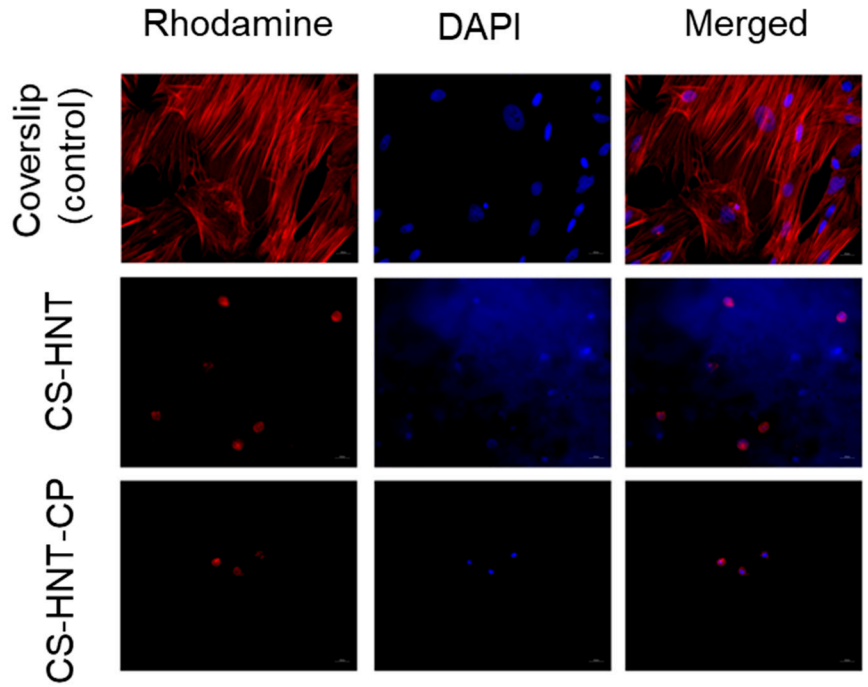


Figure 6. MSCs on surface of coverslips and electrospun mats. Magnification of 400×.

It should be noted that the number of cells in the CP-containing sample (CS-HNT-CP) was significantly lower than in the CP-free sample (CS-HNT) ($p < 0.05$) (Table 7) which is due to the ability of glucocorticoids (in therapeutic concentrations) to inhibit the proliferation and migration of various cell types, including stem cells [49]. At the same time, none of the mats tested showed a cytotoxic effect, as indicated by the absence of cells in a state of necrosis, in good agreement with the results obtained in the THP-1 cell line model (Section 3.5).

Table 7. Number of cells on the surface of the electrospun mats.

Sample	Number of Cells
CS-HNT	70.9 ± 4.0
CS-HNT-CP	13.1 ± 1.0 *

* $p < 0.05$.

4. Conclusions

Electrospun nonwovens made from the mucoadhesive natural polymer CS offer significant advantages for the delivery of topical corticosteroids directly to the oromucosal area, aiding in the treatment of various inflammatory and immunopathological conditions of the oral cavity. In this study, we investigated the pharmacotherapeutic capabilities of an electrospun mat composed of CS and doped with HNTs as an oromucosal delivery system for the controlled release of corticosteroids.

We successfully developed an electrospinning technique and identified the optimal composition of electrospinning solutions: a 2.4% solution of CS in 46% acetic acid, supplemented with 10% PEO (relative to CS mass) and 5% HNTs (also relative to CS mass). The corticosteroid CP was incorporated as an ethanol solution at a concentration of 2 mg per gram of final web. By optimizing the process parameters—an electrospinning voltage of 50–65 kV, a spinning electrode rotation speed of 10 min^{-1}, and an electrode separation of 24 cm—we obtained uniform nanofibers for both CS-HNT and CS-HNT-CP mats with mean diameters of 236 nm and 241 nm, respectively.

The CP-loaded electrospun mats exhibited impressive mechanical properties, including high strength and excellent elasticity, with a Young's modulus of 632 MPa and an ultimate deformation of 11%. They also facilitated a modified biphasic release of the corticosteroid: an initial burst release that acted as a pulsed dose, followed by a sustained release phase that maintained therapeutic levels of the drug. Notably, these nanofiber mats maintained the anti-inflammatory efficacy of the CP at levels comparable to that of free drug and did not exhibit cytotoxicity.

In conclusion, the electrospinning method developed to prepare nonwoven mats of CS doped with HNTs represents a promising approach for the preparation of biopolymer systems for topical delivery of corticosteroids.

Author Contributions: Conceptualization, N.V.D., V.A.P., and Y.A.S.; methodology, N.V.D., V.A.P., I.V.K., A.S.G., and D.N.P.; investigation, N.V.D., V.A.P., I.V.K., A.S.T., A.A.R., A.S.G., A.I.M., A.A.M., I.V.G., and D.N.P.; writing—original draft preparation, N.V.D., V.A.P., I.V.K., A.S.G., I.V.G., and D.N.P.; writing—review and editing, Y.A.S.; supervision, Y.A.S.; project administration, Y.A.S.; funding acquisition, Y.A.S. All authors have read and agreed to the published version of the manuscript.

Funding: This research was funded by the St. Petersburg Science Foundation, grant number 23-RB-03-07.

Institutional Review Board Statement: The in vitro experiments were approved by the Commission for the Control of Care and Use of Laboratory Animals at Almazov National Medical Research Centre (protocol No. 21-12PZ#V3, 13 July 2021).

Data Availability Statement: Data are contained within the article and available upon request.

Acknowledgments: The authors thank Ilya Serov (Inmed Ltd., St. Petersburg, Russia) and Elena Ivan'kova (Institute of Macromolecular Compounds, St. Petersburg, Russia) for performing SEM experiments on the electrospun mats and halloysite nanotubes, respectively.

Conflicts of Interest: The authors declare no conflicts of interest.

References

1. Dott, C.; Tyagi, C.; Tomar, L.K.; Choonara, Y.E.; Kumar, P.; du Toit, L.C.; Pillay, V. A mucoadhesive electrospun nanofibrous matrix for rapid oramucosal drug delivery. *J. Nanomater.* **2013**, *2013*, 924947. [CrossRef]
2. Dubashynskaya, N.V.; Petrova, V.A.; Skorik, Y.A. Biopolymer drug delivery systems for oromucosal application: Recent trends in pharmaceutical r&d. *Int. J. Mol. Sci.* **2024**, *25*, 5359. [CrossRef] [PubMed]
3. Vega-Avila, A.L.; Perales-Perez, O.; Valentín Rullan, R. Biopolymers nanofibers for biomedical applications and environmental applications. In *Electrospun Biomaterials and Related Technologies*; Springer: Berlin/Heidelberg, Germany, 2017; pp. 109–147.
4. Luraghi, A.; Peri, F.; Moroni, L. Electrospinning for drug delivery applications: A review. *J. Control. Release* **2021**, *334*, 463–484. [CrossRef] [PubMed]
5. Narayanaswamy, R.; Torchilin, V.P. Hydrogels and their applications in targeted drug delivery. In *The Road from Nanomedicine to Precision Medicine*; Taylor & Francis Group: Abingdon, UK, 2020; pp. 1117–1150.
6. Eslamian, M.; Khorrami, M.; Yi, N.; Majd, S.; Abidian, M.R. Electrospinning of highly aligned fibers for drug delivery applications. *J. Mater. Chem. B* **2019**, *7*, 224–232. [CrossRef]
7. Wang, J.; Windbergs, M. Controlled dual drug release by coaxial electrospun fibers–impact of the core fluid on drug encapsulation and release. *Int. J. Pharm.* **2019**, *556*, 363–371. [CrossRef] [PubMed]
8. Nikmaram, N.; Roohinejad, S.; Hashemi, S.; Koubaa, M.; Barba, F.J.; Abbaspourrad, A.; Greiner, R. Emulsion-based systems for fabrication of electrospun nanofibers: Food, pharmaceutical and biomedical applications. *RSC Adv.* **2017**, *7*, 28951–28964. [CrossRef]
9. Opriș, O.; Mormile, C.; Lung, I.; Stegarescu, A.; Soran, M.-L.; Soran, A. An overview of biopolymers for drug delivery applications. *Appl. Sci.* **2024**, *14*, 1383. [CrossRef]
10. Fazio, E.; Ridolfo, A.; Neri, G. Thermally activated noble metal nanoparticles incorporated in electrospun fiber-based drug delivery systems. *Curr. Nanomater.* **2019**, *4*, 21–31. [CrossRef]
11. Wan, X.; Li, P.; Jin, X.; Su, F.; Shen, J.; Yuan, J. Poly (ε-caprolactone)/keratin/heparin/vegf biocomposite mats for vascular tissue engineering. *J. Biomed. Mater. Res. Part A* **2020**, *108*, 292–300. [CrossRef]
12. Olsson, R.T.; Kraemer, R.; Lopez-Rubio, A.; Torres-Giner, S.; Ocio, M.J.; Lagarón, J.M. Extraction of microfibrils from bacterial cellulose networks for electrospinning of anisotropic biohybrid fiber yarns. *Macromolecules* **2010**, *43*, 4201–4209. [CrossRef]
13. Somord, K.; Somord, K.; Suwantong, O.; Thanomsilp, C.; Peijs, T.; Soykeabkaew, N. Self-reinforced poly (lactic acid) nanocomposites with integrated bacterial cellulose and its surface modification. *Nanocomposites* **2018**, *4*, 102–111. [CrossRef]
14. Pereira, A.G.; Fajardo, A.R.; Gerola, A.P.; Rodrigues, J.H.; Nakamura, C.V.; Muniz, E.C.; Hsieh, Y.-L. First report of electrospun cellulose acetate nanofibers mats with chitin and chitosan nanowhiskers: Fabrication, characterization, and antibacterial activity. *Carbohydr. Polym.* **2020**, *250*, 116954. [CrossRef] [PubMed]
15. Naseri, N.; Algan, C.; Jacobs, V.; John, M.; Oksman, K.; Mathew, A.P. Electrospun chitosan-based nanocomposite mats reinforced with chitin nanocrystals for wound dressing. *Carbohydr. Polym.* **2014**, *109*, 7–15. [CrossRef]
16. Jalvandi, J.; White, M.; Truong, Y.B.; Gao, Y.; Padhye, R.; Kyratzis, I.L. Release and antimicrobial activity of levofloxacin from composite mats of poly (*E*-caprolactone) and mesoporous silica nanoparticles fabricated by core–shell electrospinning. *J. Mater. Sci.* **2015**, *50*, 7967–7974. [CrossRef]
17. Zhou, X.; Chen, L.; Wang, W.; Jia, Y.; Chang, A.; Mo, X.; Wang, H.; He, C. Electrospun nanofibers incorporating self-decomposable silica nanoparticles as carriers for controlled delivery of anticancer drug. *RSC Adv.* **2015**, *5*, 65897–65904. [CrossRef]
18. Mortimer, C.J.; Wright, C.J. The fabrication of iron oxide nanoparticle-nanofiber composites by electrospinning and their applications in tissue engineering. *Biotechnol. J.* **2017**, *12*, 1600693. [CrossRef]
19. Petrova, V.A.; Poshina, D.N.; Golovkin, A.S.; Mishanin, A.I.; Zhuravskii, S.G.; Yukina, G.Y.; Naumenko, M.Y.; Sukhorukova, E.G.; Savin, N.A.; Erofeev, A.S. Electrospun composites of chitosan with cerium oxide nanoparticles for wound healing applications: Characterization and biocompatibility evaluation in vitro and in vivo. *Polymers* **2024**, *16*, 1787. [CrossRef] [PubMed]
20. Zienkiewicz-Strzałka, M.; Deryło-Marczewska, A.; Skorik, Y.A.; Petrova, V.A.; Choma, A.; Komaniecka, I. Silver nanoparticles on chitosan/silica nanofibers: Characterization and antibacterial activity. *Int. J. Mol. Sci.* **2019**, *21*, 166. [CrossRef] [PubMed]
21. Fahimizadeh, M.; Wong, L.W.; Baifa, Z.; Sadjadi, S.; Auckloo, S.A.B.; Palaniandy, K.; Pasbakhsh, P.; Tan, J.B.L.; Singh, R.R.; Yuan, P. Halloysite clay nanotubes: Innovative applications by smart systems. *Appl. Clay Sci.* **2024**, *251*, 107319. [CrossRef]
22. Toledano-Magaña, Y.; Flores-Santos, L.; de Oca, G.M.; González-Montiel, A.; García-Ramos, J.-C.; Mora, C.; Saavedra-Ávila, N.-A.; Gudiño-Zayas, M.; González-Ramírez, L.-C.; Laclette, J.P.; et al. Toxicological evaluations in macrophages and mice acutely and chronically exposed to halloysite clay nanotubes functionalized with polystyrene. *ACS Omega* **2021**, *6*, 29882–29892. [CrossRef] [PubMed]
23. Danyliuk, N.; Tomaszewska, J.; Tatarchuk, T. Halloysite nanotubes and halloysite-based composites for environmental and biomedical applications. *J. Mol. Liq.* **2020**, *309*, 113077. [CrossRef]

24. Mobaraki, M.; Karnik, S.; Li, Y.; Mills, D.K. Therapeutic applications of halloysite. *Appl. Sci.* **2021**, *12*, 87. [CrossRef]
25. Wong, L.W.; Pasbakhsh, P.; Arabi, A.M.; Keeling, J.; Tan, J.B.L. Halloysite nanotubes from various geological deposits: New insights to acid etching and their impacts on products' characteristics. *J. Environ. Chem. Eng.* **2021**, *9*, 106235. [CrossRef]
26. Tohidi, S.; Ghaee, A.; Barzin, J. Preparation and characterization of poly (lactic-co-glycolic acid)/chitosan electrospun membrane containing amoxicillin-loaded halloysite nanoclay. *Polym. Adv. Technol.* **2016**, *27*, 1020–1028. [CrossRef]
27. Saleh, M.Y.; Prajapati, N.; DeCoster, M.A.; Lvov, Y. Tagged halloysite nanotubes as a carrier for intercellular delivery in brain microvascular endothelium. *Front. Bioeng. Biotechnol.* **2020**, *8*, 451. [CrossRef] [PubMed]
28. CeCe, R.; Jining, L.; Islam, M.; Korvink, J.G.; Sharma, B. An overview of the electrospinning of polymeric nanofibers for biomedical applications related to drug delivery. *Adv. Eng. Mater.* **2024**, *26*, 2301297. [CrossRef]
29. Dubashynskaya, N.V.; Skorik, Y.A. Patches as polymeric systems for improved delivery of topical corticosteroids: Advances and future perspectives. *Int. J. Mol. Sci.* **2022**, *23*, 12980. [CrossRef] [PubMed]
30. Sofi, H.S.; Abdal-Hay, A.; Ivanovski, S.; Zhang, Y.S.; Sheikh, F.A. Electrospun nanofibers for the delivery of active drugs through nasal, oral and vaginal mucosa: Current status and future perspectives. *Mater. Sci. Eng. C* **2020**, *111*, 110756. [CrossRef] [PubMed]
31. Wydro, P.; Krajewska, B.; Hac-Wydro, K. Chitosan as a lipid binder: A langmuir monolayer study of chitosan− lipid interactions. *Biomacromolecules* **2007**, *8*, 2611–2617. [CrossRef]
32. Muzzarelli, R.; Frega, N.; Miliani, M.; Muzzarelli, C.; Cartolari, M. Interactions of chitin, chitosan, n-lauryl chitosan and n-dimethylaminopropyl chitosan with olive oil. *Carbohydr. Polym.* **2000**, *43*, 263–268. [CrossRef]
33. Moeini, A.; Pedram, P.; Makvandi, P.; Malinconico, M.; d'Ayala, G.G. Wound healing and antimicrobial effect of active secondary metabolites in chitosan-based wound dressings: A review. *Carbohydr. Polym.* **2020**, *233*, 115839. [CrossRef] [PubMed]
34. Wu, Y.; Zhang, Y.; Ju, J.; Yan, H.; Huang, X.; Tan, Y. Advances in halloysite nanotubes–polysaccharide nanocomposite preparation and applications. *Polymers* **2019**, *11*, 987. [CrossRef]
35. Said, Z.; Murdoch, C.; Hansen, J.; Siim Madsen, L.; Colley, H.E. Corticosteroid delivery using oral mucosa equivalents for the treatment of inflammatory mucosal diseases. *Eur. J. Oral Sci.* **2021**, *129*, e12761. [CrossRef]
36. Colley, H.; Said, Z.; Santocildes-Romero, M.; Baker, S.; D'Apice, K.; Hansen, J.; Madsen, L.S.; Thornhill, M.; Hatton, P.; Murdoch, C. Pre-clinical evaluation of novel mucoadhesive bilayer patches for local delivery of clobetasol-17-propionate to the oral mucosa. *Biomaterials* **2018**, *178*, 134–146. [CrossRef]
37. Gonzalez-Moles, M.A.; Morales, P.; Rodriguez-Archilla, A.; Isabel, I.R.-A.; Gonzalez-Moles, S. Treatment of severe chronic oral erosive lesions with clobetasol propionate in aqueous solution. *Oral Surg. Oral Med. Oral Pathol. Oral Radiol. Endodontol.* **2002**, *93*, 264–270. [CrossRef]
38. Zvidzayi, M.; Rath, S.; Bon, C.; Abboo, S.; Kanfer, I. A novel approach to assess the potency of topical corticosteroids. *Pharmaceutics* **2021**, *13*, 1456. [CrossRef] [PubMed]
39. Pogodina, N.; Pavlov, G.; Bushin, S.; Mel'Nikov, A.; Lysenko, Y.B.; Nud'Ga, L.; Marsheva, V.; Marchenko, G.; Tsvetkov, V. Conformational characteristics of chitosan molecules as demonstrated by diffusion-sedimentation analysis and viscometry. *Polym. Sci. USSR* **1986**, *28*, 251–259. [CrossRef]
40. Marques, M.R.; Loebenberg, R.; Almukainzi, M. Simulated biological fluids with possible application in dissolution testing. *Dissolution Technol.* **2011**, *18*, 15–28. [CrossRef]
41. Dubashynskaya, N.V.; Bokatyi, A.N.; Trulioff, A.S.; Rubinstein, A.A.; Kudryavtsev, I.V.; Skorik, Y.A. Development and bioactivity of zinc sulfate cross-linked polysaccharide delivery system of dexamethasone phosphate. *Pharmaceutics* **2023**, *15*, 2396. [CrossRef]
42. Petrova, V.A.; Khripunov, A.K.; Golovkin, A.S.; Mishanin, A.I.; Gofman, I.V.; Romanov, D.P.; Migunova, A.V.; Arkharova, N.A.; Klechkovskaya, V.V.; Skorik, Y.A. Bacterial cellulose (komagataeibacter rhaeticus) biocomposites and their cytocompatibility. *Materials* **2020**, *13*, 4558. [CrossRef]
43. Poshina, D.N.; Khadyko, I.A.; Sukhova, A.A.; Serov, I.V.; Zabivalova, N.M.; Skorik, Y.A. Needleless electrospinning of a chitosan lactate aqueous solution: Influence of solution composition and spinning parameters. *Technologies* **2019**, *8*, 2. [CrossRef]
44. Peppas, N.A.; Sahlin, J.J. Hydrogels as mucoadhesive and bioadhesive materials: A review. *Biomaterials* **1996**, *17*, 1553–1561. [CrossRef] [PubMed]
45. Devi, N.; Dutta, J. Development and in vitro characterization of chitosan/starch/halloysite nanotubes ternary nanocomposite films. *Int. J. Biol. Macromol.* **2019**, *127*, 222–231. [CrossRef]
46. Boucard, N.; Viton, C.; Domard, A. New aspects of the formation of physical hydrogels of chitosan in a hydroalcoholic medium. *Biomacromolecules* **2005**, *6*, 3227–3237. [CrossRef] [PubMed]
47. Darbasi, M.; Askari, G.; Kiani, H.; Khodaiyan, F. Development of chitosan based extended-release antioxidant films by control of fabrication variables. *Int. J. Biol. Macromol.* **2017**, *104*, 303–310. [CrossRef] [PubMed]

48. Kowalonek, J. Surface and thermal behavior of chitosan/poly (ethylene oxide) blends. *Mol. Cryst. Liq. Cryst.* **2016**, *640*, 78–89. [CrossRef]
49. Wang, Y.; Luan, S.; Yuan, Z.; Lin, C.; Fan, S.; Wang, S.; Ma, C.; Wu, S. Therapeutic effect of platelet-rich plasma on glucocorticoid-induced rat bone marrow mesenchymal stem cells in vitro. *BMC Musculoskelet. Disord.* **2022**, *23*, 151.

Disclaimer/Publisher's Note: The statements, opinions and data contained in all publications are solely those of the individual author(s) and contributor(s) and not of MDPI and/or the editor(s). MDPI and/or the editor(s) disclaim responsibility for any injury to people or property resulting from any ideas, methods, instructions or products referred to in the content.